

# Structure of a Novel Cofactor Containing N-(7-Mercaptoheptanoyl)-O-3-phosphothreonine<sup>†</sup>

Frank D. Sauer,\*<sup>‡</sup> Barbara A. Blackwell,<sup>§</sup> John K. G. Kramer,<sup>†</sup> and Brian J. Marsden<sup>||</sup>

Animal Research Centre and Plant Research Centre, Research Branch, Agriculture Canada, Ottawa, Ontario, Canada K1A 0C6,  
and National Research Council, Ottawa, Ontario, Canada

Received March 7, 1990; Revised Manuscript Received May 8, 1990

**ABSTRACT:** The cofactor required in the methylcoenzyme M methylreductase reaction was shown to be a large molecule with an  $M_r$  of 1149.21 in the free acid form. The cofactor, named MRF for methyl reducing factor, was identified from analyses by fast atom bombardment mass spectrometry and <sup>1</sup>H, <sup>13</sup>C, and <sup>31</sup>P NMR spectroscopy as uridine 5'-[N-(7-mercaptoheptanoyl)-O-3-phosphothreonine-P-yl(2-acetamido-2-deoxy-β-mannopyranuronosyl)(acid anhydride)]-(1→4)-O-2-acetamido-2-deoxy-α-glucopyranosyl diphosphate. MRF contains N-(7-mercaptoheptanoyl)threonine O-3-phosphate (HS-HTP) [Noll, K. M., Rinehart, K. L., Tanner, R. S., & Wolfe, R. S. (1986) *Proc. Natl. Acad. Sci. U.S.A.* 83, 4238-4242] and is linked to C-6 of 2-acetamido-2-deoxymannopyranuronic acid of the UDP-disaccharide through a carboxylic-phosphoric anhydride linkage. It is postulated that this bond is responsible for the instability of the molecule and its hydrolysis during isolation. Analyses of Eadie and Hofstee plots of the methylcoenzyme M methylreductase reaction indicate that MRF has a 6-fold lower  $K_{m(app)}$  than HS-HTP and a 50% greater  $V_{max}$ . This suggests that the UDP-disaccharide moiety may be of importance in the binding of MRF to the enzyme active site.

In the stepwise reduction of CO<sub>2</sub> to methane, the terminal enzyme, methylcoenzyme M methylreductase, has an absolute requirement for a novel cofactor, N-(7-mercaptoheptanoyl)-threonine O-3-phosphate (HS-HTP) (Noll et al., 1986). It was recognized early that HS-HTP might be part of a larger molecule that breaks down during isolation and purification (Sauer et al., 1984; Noll & Wolfe, 1986). It was found that while HS-HTP as the free thiol has a molecular weight of 343, the natural cofactor isolated from cell extracts of *Methanobacterium thermoautotrophicum* was completely retained by Amicon UM2 Diaflo ultrafilters, which have a molecular weight cutoff of approximately 1000 (Sauer et al., 1984). It was noted further that during the isolation process the natural cofactor hydrolyzed into two breakdown products, one of which was identified as uridine 5'-(2-acetamido-2-deoxy-β-mannopyranuronosyl)-(1→4)-O-2-acetamido-2-deoxy-α-glucopyranosyl diphosphate (UDP-GlcNAc-ManNAcA) (Marsden et al., 1989) and the other as HS-HTP. It was postulated that in the naturally occurring bacterial cofactor, HS-HTP is linked through the phosphate group to C-6 of N-acetylmannosaminuronic acid. Here we present results which show that the elemental formula of the intact molecule is C<sub>36</sub>H<sub>58</sub>O<sub>29</sub>N<sub>5</sub>P<sub>3</sub>S with an  $M_r$  of 1149.21. The structure has been determined by NMR and mass spectroscopic analyses. The name proposed for this cofactor is methyl reducing factor or MRF.

## MATERIALS AND METHODS

**MRF Preparation.** Cells of *Mb. thermoautotrophicum* were cultured (Marsden et al., 1989), harvested, and stored as described previously (Sauer et al., 1984; Sauer et al., 1986).

All subsequent operations were carried out with strict exclusion of O<sub>2</sub> either in an anaerobic chamber (Coy Laboratory Products, Ann Arbor, MI) or in sealed tubes. In preliminary experiments, cells were disrupted either by ultrasound or in a Ribi cell fractionator (Norwalk CT) (Sauer et al., 1984). Subsequently it was found that MRF could be isolated equally well from cells disrupted by autoclaving, so for convenience, this procedure was used. The cells (120 g wet wt) were resuspended in 5 mM potassium phosphate buffer, pH 7.0 (1 g/2 mL), autoclaved for 15 min at 121 °C, cooled, and adjusted to pH 2.5-3.0 with 2 N HCl. Denatured protein and cell debris were removed by centrifugation and the tan-colored, acid-treated supernatant (ATS) was adjusted to pH 7.0 with 2 N NaOH. The ATS was applied to a DEAE-Sephadex A-25 column (5 × 52 cm) and washed with 5 mM potassium phosphate buffer (pH 7.0) until no more colored impurities were eluted. All buffers and chromatography columns were reduced with 10 mM 2-mercaptoethanol. The MRF containing fraction was eluted with a linear gradient of 0-1 M NaCl (4 L) in 5 mM potassium phosphate buffer (pH 7.0) at a flow rate of 6 mL/min. MRF was eluted between fraction 130 and 150 (18 mL/fraction). MRF activity was detected by CH<sub>4</sub> synthesis in the methylcoenzyme M methylreductase assay (Sauer et al., 1986). At this step in the procedure, the fractions that contain MRF are brown in color and contain all of the methanopterin. These fractions were pooled, concentrated, and repeatedly washed in a 200-mL Amicon stirred cell with a YCO5 membrane ( $M_r$  500 cutoff). The desalted sample was applied to a second DEAE-Sephadex A-25, column (2.5 × 12 cm) and washed with 7 mM HCl until methanopterin and a brown fraction were eluted. MRF remained on the column as a light colored yellow-green band, which was subsequently eluted with a linear gradient of 0-0.6 M NaCl (600 mL). MRF containing fractions were detected with the methylcoenzyme M methylreductase assay and again pooled and desalted by ultrafiltration. MRF was applied to a third DEAE-Sephadex A-25 column (2.5 × 25 cm) and eluted with a linear gradient of 0-0.6 M NaCl (1 L). At this stage of purification, MRF could be detected by the UDP UV ab-

<sup>†</sup> This is Contribution No. 1671 from the ARC and Contribution No. 1249 from the PRC.

\* To whom correspondence should be addressed.

<sup>‡</sup> Animal Research Centre, Agriculture Canada.

<sup>§</sup> Plant Research Centre, Agriculture Canada.

<sup>||</sup> National Research Council. Current address: Clinical Research Institute of Montreal, Montreal, Quebec, Canada H2W 1R7.

sorption at 260 nm, which coincided with MRF activity. After desalting, MRF was lyophilized and stored in sealed glass ampules at  $-20^{\circ}\text{C}$  under vacuum. When necessary, the hydrolysis product, HS-HTP, was removed from MRF by chromatography on a hydroxylapatite column ( $15 \times 2.5$  cm) (Bio-Rad, Richmond, CA). The desalted sample was applied in 5 mM potassium phosphate buffer pH 7.0 containing 10 mM 2-mercaptoethanol, which also served as the eluting buffer. With a flow rate of 0.7 mL/min, MRF was eluted in fractions 18–22 (4 mL/fraction). HS-HTP free of UDP-disaccharide was eluted in fractions 37–50.

**Carbohydrate Isolation.** The carbohydrate moiety was isolated by acid hydrolysis of MRF on a DEAE-Sephadex column as described (Marsden et al., 1989). The hydrolytic fragment, UDP-GlcNAc-ManNAcA, was isolated in pure form after elution with a linear gradient of NaCl.

**MRF Purity.** HS-HTP was synthesized as described (Sauer et al., 1987) and used as a standard for measuring  $R_f$  values. MRF and HS-HTP were separated on 500- $\mu\text{m}$  silica gel G plates (Analtech, Newark, DE) in a solvent system of (1) 1-butanol-methanol-water-concentrated ammonium hydroxide (60:20:20:1) or (2) 1-butanol-acetic acid-water (4:1:1) with  $R_f$  values of 0.07 and 0.48 (solvent system 1) and 0.15 and 0.40 (solvent system 2), respectively. MRF and HS-HTP were also separated on crystalline cellulose plates (Avicel F; Analtech, Newark, DE) with a solvent system of pyridine-ethyl acetate-acetic acid-water (36:36:7:2) ( $R_f$  0.16 and 0.63, respectively). With high-voltage paper electrophoresis (2 h at 1250 V) in pyridine-acetic acid-water (25:1:220), MRF migrates ahead of HS-HTP toward the anode. Detection of MRF and HS-HTP on paper and silica gel plates was by a 1.5% methanolic sodium nitroprusside spray for SH groups followed by a 2% sodium cyanide methanolic spray for SS groups.

**Methylcoenzyme M Methylreductase Assay.** Methylcoenzyme M methylreductase, a high molecular weight enzyme, which has recently been shown (Mayer et al., 1988) to be structured into membrane-bound large spherical bodies, was isolated as described previously (Sauer et al., 1984) under method 1. The enzyme was stable for months without any appreciable loss in activity when stored anaerobically in ice. Enzyme assays were done in a 0.4-mL volume in 1-mL Reacti-Vials (Pierce Chemical Co., Rockford IL) and  $\text{CH}_4$  production was measured as described (Sauer et al., 1986). To measure kinetic constants, the reaction mixture contained enzyme protein, 1.2 mg; ATP, 2.5 mM;  $\text{Mg}^{2+}$ , 3.0 mM; methylcoenzyme M, 2.5 mM; KCl, 25 mM; potassium phosphate (pH 7.0), 25 mM; and MRF or HS-HTP as indicated. The enzyme was incubated for 10 and 20 min with constant shaking in a water bath at  $60^{\circ}\text{C}$ .

**NMR Spectroscopy.** Samples for NMR analysis were lyophilized twice from  $\text{D}_2\text{O}$  and were dissolved in  $\text{D}_2\text{O}$  at pD 8.7 (uncorrected reading with a combination glass electrode) and sealed in 5-mm NMR tubes under  $\text{N}_2$ .

$^1\text{H}$ ,  $^{13}\text{C}$ , and  $^{31}\text{P}$  NMR spectra were recorded at 500.13, 125.2, and 202.4 MHz, respectively, on a Bruker AM500 NMR spectrometer operating at 303 K. The pulse sequence for the 1-D rotating frame nuclear Overhauser enhancement (rOe) experiment was derived from that described by Kessler et al. (1987) for the 2-D ROESY experiment. This experiment was performed on a Varian VXR-400S NMR spectrometer operating at 399.95 MHz and 298 K.

Chemical shifts were referenced to external TSP for  $^1\text{H}$  and 85%  $\text{H}_3\text{PO}_4$  for  $^{31}\text{P}$ .  $^{13}\text{C}$  chemical shifts were referenced to external dioxane at 67.4 ppm and reported relative to TMS.

Spectra were recorded by using a 5-mm triple-tuned probe under the following conditions: for  $^1\text{H}$  spectra, a 5-KHz spectral window, 32K data points, a  $10\ \mu\text{s}$  ( $60^{\circ}$ ) pulse, and a 4.5-s recycle time; for  $^{13}\text{C}$  spectra, 32K data points, a 24-KHz spectral window,  $8\text{-}\mu\text{s}$  ( $60^{\circ}$ ) pulse, and a 3.6-s recycle time; and for  $^{31}\text{P}$  spectra, 16K data points, a 10-KHz spectral window,  $12\text{-}\mu\text{s}$  ( $45^{\circ}$ ) pulse, and 2-s recycle time.

$^1\text{H}$  spin systems were assigned by using homonuclear correlation (COSY) spectra (Bax & Freeman, 1981), one-step relayed coherence transfer (RELAY) (Bax & Drobny, 1985), and phase-sensitive DQF-COSY (Shaka & Freeman, 1983). 2-D experiments were recorded as 512 FID's of 2K data points, using a  $90^{\circ}$  pulse of  $16\ \mu\text{s}$  and a sweepwidth of 4 KHz. Weighting functions used were sine bell squared for COSY and RELAY and a cosine bell for DQF-COSY. The data matrix was zero-filled in F1 for a final digit at a resolution of 2.7 Hz/pt.

$^{13}\text{C}$  spin systems were assigned by using DEPT and CHORTLE (Pearson, 1985) experiments, as well as by comparison to an authentic sample of UDP-*N*-acetyl glucosamine (Sigma Chemical Co., St. Louis, MO). The latter was unambiguously assigned by  $^1\text{H}$ - $^{13}\text{C}$  heteronuclear correlation (HETCOR), using 256 FID's of 4K data points, a  $90^{\circ}$  pulse of  $12\ \mu\text{s}$ , and sweepwidths of 12 KHz ( $^{13}\text{C}$ ) and 4 KHz ( $^1\text{H}$ ). The data matrix was processed using a cosine bell squared function, zero-filling in F1 and plotted as a power spectrum.

The rOe difference spectrum was obtained as follows: A selective  $180^{\circ}$  pulse using the decoupler transmitter was applied to the anomeric proton resonance of the ManNAcA sugar residue on alternate scans; coaddition of the scans in computer memory resulted in the difference spectrum. A total of 2048 scans were collected by using a spin lock period of 250 ms. The difference spectrum was resolution enhanced by using a Lorentzian to Gaussian function prior to Fourier transformation.

Spectral simulations were performed with the Bruker PANIC program.  $^1\text{H}$ - $^{31}\text{P}$  couplings were introduced by creating an extra spin of  $J_{\text{P,H}}$  at frequency 0.

**Mass Spectroscopy.** Positive-ion fast atom bombardment mass spectra (FAB-MS) were recorded on a Finnigan MAT 312 mass spectrometer in the mass range  $m/z$  490–1520. FAB mass spectra were obtained on samples of UDP-GlcNAc-ManNAcA dissolved in glycerol or MRF dissolved in thio-glycerol (3-mercapto-1,2-propanediol).

## RESULTS

A sample of MRF judged to be pure by high-voltage paper electrophoresis and silica gel TLC was used for NMR analysis. The 500-MHz  $^1\text{H}$  NMR spectrum (303 K) showed characteristic signals for two *N*-acetyl groups at 2.01 ppm (s, 3 H) and 2.02 ppm (s, 3 H), as well as a doublet attributable to a methyl group at 1.26 ppm and aliphatic methylene groups between 1.4 and 2.8 ppm (Table I). The presence of three sugar units is indicated by three signals attributable to anomeric protons at 5.93, 5.44, and 4.86 ppm, as well as overlapping multiplets between 3.50 and 4.50 ppm. While two of the anomeric proton resonances appear as doublets (5.93 ppm,  $J = 3.7$  Hz, and 4.86 ppm,  $J = 1.6$  Hz), the third at 5.44 ppm appears as a quartet, the larger splitting of 7.3 Hz being attributable to coupling to a phosphate moiety. Two additional doublets at 5.90 and 7.90 ppm form an isolated double bond system and were assigned to H-5 and H-6 of the uracil ring.

The  $^{13}\text{C}$  NMR data were obtained with UDP-GlcNAc-ManNAcA (Figure 1A) and a mixture of UDP-GlcNAc-ManNAcA and MRF (Figure 1B). The  $^{13}\text{C}$  NMR spectrum (Figure 1) confirmed the presence of three sugar moieties, two

Table 1: 500-MHz  $^1\text{H}$  NMR Chemical Shift Assignments for MRF, UDP-GlcNAc-ManNAcA, HS-HTP, and UDP-GlcNAc Standard

position	MRF	UDP-GlcNAc-ManNAcA <sup>a</sup>	UDP-GlcNAc
uracil			
5	5.90	5.87 (5, 6 = 8.0) <sup>b</sup>	5.93 (5, 6 = 8.1)
6	7.90 (5, 6 = 8.2)	7.87	7.90
ribose			
1	5.93	5.88 (1, 2 = 3.7)	5.94 (1, 2 = 4.0)
2	4.44	4.26 (2, 3 = 4.5)	4.32 (2, 3 = 5.2)
3	4.46	4.27	4.33
4	4.23	4.18 (4, 5 = 2.6; 4, 5' = 3.1)	4.25 (4, 5 = 2.6; 4, 5' = 3.1)
5	4.20	4.14 (5, P = 4.5)	4.20 (5, P = 4.3)
5'	4.10	4.08 (5'P = 5.6)	4.14 (5', P = 5.4)
GlcNAc			
1	5.44 (1, 2 = 3.3; 1, P = 7.1)	5.40 (1, 2 = 3.3; 1, P = 7.3)	5.47 (1, 2 = 3.3; 1, P = 7.3)
2	3.94	3.90 (2, 3 = 10.5; 2, P = 3.0)	3.95 (2, 3 = 10.4; 2, P = 3.0)
3	3.84 (3, 4 = 8.8)	3.80 (3, 4 = 8.8)	3.76 (3, 4 = 9.1)
4	3.71 (4, 5 = 9.4)	3.68 (4, 5 = 10.0)	3.50 (4, 5 = 9.8)
5	3.90	3.85 (2, 3 = 10.5; 2, P = 3.0)	3.95 (5, 6 = 2.3; 5, 6' = 4.3)
6	3.77 (6, 6' = 13.4)	3.72 (6, 6' = 12.5)	3.83 (6, 6' = 12.5)
6'	3.69 (5,6' = 3.9)	3.64	3.75
NAc	2.01	1.98	2.03
ManNAcA			
1	4.86 (1, 2 = 1.6)	4.82 (1, 2 = 1.5)	
2	4.50 (2, 3 = 4.4)	4.45 (2, 3 = 4.2)	
3	3.81 (3, 4 = 8.8)	3.73 (3, 4 = 9.9)	
4	3.54 (4, 5 = 9.9)	3.49 (4, 5 = 9.8)	
5	3.70 (5, 4 = 9.9)	3.65	
NAc	2.02	2.00	

position	MRF	HS-HTP
threonine		
2	4.54	4.55 (2, 3 = 2.4; 2, P = 2.0)
3	5.32 (3, 2 = 1.7; 3, P = 7.6)	4.84 (3, 4 = 6.4)
4	1.26 (4, 3 = 6.1)	1.30 (4, 3 = 6.4)
heptanoic acid		
2	2.50	2.36 (A, B = 14.9; 2, 3 = 7.1)
3	1.57 <sup>c</sup>	1.64
4	1.36 <sup>c</sup>	1.36
5	1.36 <sup>c</sup>	1.39
6	1.57 <sup>c</sup>	1.64
7	2.84 (7, 6 = 6.6)	2.72 (7, 6 = 7.1)

<sup>a</sup> From Marsden et al. (1989). <sup>b</sup>  $^1\text{H}/^1\text{H}$  coupling constants in hertz. <sup>c</sup> Not resolvable.

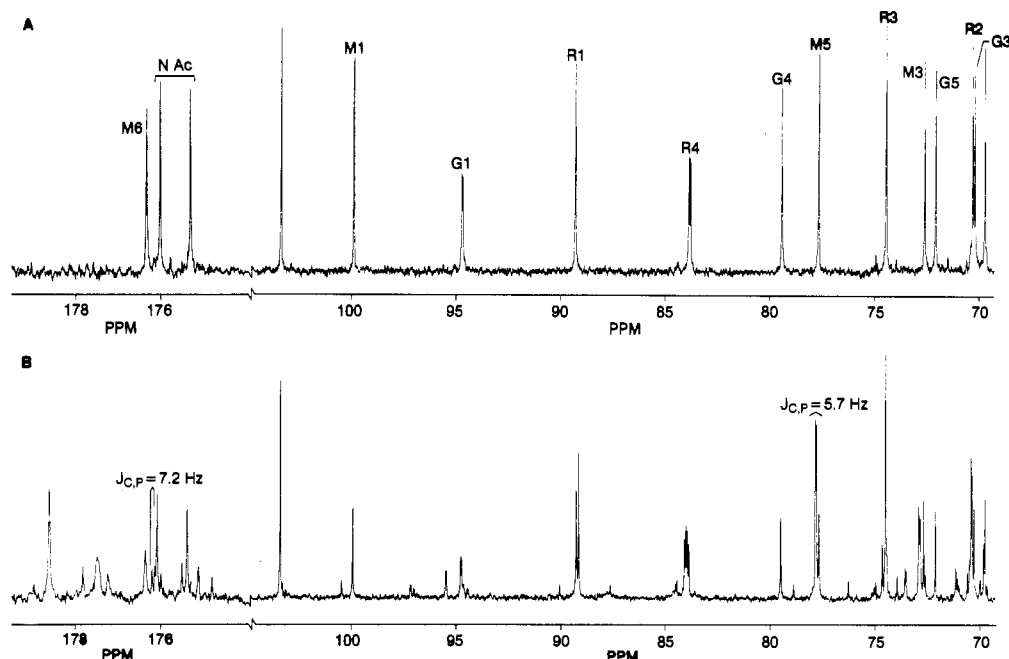


FIGURE 1: Comparison of the carbonyl and carbohydrate regions of the 125-MHz  $^{13}\text{C}$  NMR spectra of (A) UDP-GlcNAc-ManNAcA and (B) MRF. The resonances in (A) are assigned to the individual carbons of uridine (U), GlcNAc (G), ribose (R), and ManNAcA (M). In the MRF spectrum, resonances due to UDP-GlcNAc-ManNAcA can be seen. The carbon-phosphorus coupling due to the anhydride linkage between threonine phosphate and C-6 of the ManNAcA residue can be observed at M5 and M6. The additional resonance at 178.6 ppm is assigned to the carbonyl group of the heptanoic acid function.

hexoses and one pentose, from the 16 resonances occurring between 50 and 100 ppm. Three anomeric carbon resonances

are present at 89.1, 95.5, and 100.0 ppm, the second appearing as a doublet due to  $^{13}\text{C}$ - $^{31}\text{P}$  coupling ( $J_{\text{C,P}} = 5.4$  Hz). Four

Table II: 125-MHz  $^{13}\text{C}$  NMR Chemical Shift Assignments (ppm from TMS)

position	MRF	UDP-GlcNAc-ManNAc <sup>a</sup>	UDP-GlcNAc
uracil			
2	152.5	152.6	151.9
4	166.8	167.0	166.3
5	103.4	103.4	102.8
6	142.3	142.4	141.6
ribose			
1	89.1	89.3	88.5
2	70.3	70.3	73.8
3	74.6	74.6	69.7
4	83.8 ( $^3J_{\text{C,P}} = 9.0$ Hz)	84.0 ( $^3J_{\text{C,P}} = 8.9$ Hz)	83.3 ( $^3J_{\text{C,P}} = 9.0$ Hz)
5	65.5 ( $^2J_{\text{C,P}} = 4.5$ Hz)	65.7 ( $^2J_{\text{C,P}} = 5.4$ Hz)	65.0 ( $^2J_{\text{C,P}} = 5.4$ Hz)
GlcNAc			
1	95.5 ( $^2J_{\text{C,P}} = 5.4$ Hz)	94.8 ( $^2J_{\text{C,P}} = 4.5$ Hz)	94.5 ( $^2J_{\text{C,P}} = 6.3$ Hz)
2	54.1 ( $^3J_{\text{C,P}} = 9.0$ Hz)	54.1 ( $^3J_{\text{C,P}} = 9.0$ Hz)	53.7 ( $^3J_{\text{C,P}} = 8.3$ Hz)
3	70.2	70.2	71.0
4	79.0	79.5	69.6
5	72.1	72.1	73.1
6	60.5	60.5	60.4
Ac	22.7	22.8	22.1
C=O	175.5	175.4	174.8
ManNAc			
1	100.0	100.0	
2	53.8	53.8	
3	72.7	72.7	
4	69.8	69.7	
5	77.8 ( $^3J_{\text{C,P}} = 5.7$ Hz)	77.6	
6	176.3 ( $^2J_{\text{C,P}} = 7.2$ Hz)	176.4	
Ac	22.7	22.8	
C=O	176.2	176.2	

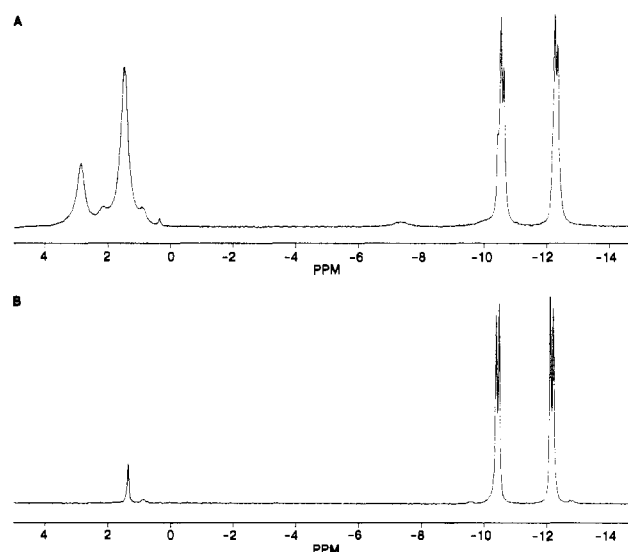
  

position	MRF	HS-HTP <sup>b</sup>
heptanoic acid		
1	178.6	175.8
2	33.5	33.3
3	24.4	23.2
4	27.8	25.7
5	28.5	26.1
6	25.9	25.1
7	36.4	36.2
phosphothreonine		
1	177.5	171.0
2	64.4 ( $^3J_{\text{C,P}} = 9.0$ Hz)	55.1 ( $^3J_{\text{C,P}} = 7.2$ Hz)
3	72.8 ( $^2J_{\text{C,P}} = 8.1$ Hz)	70.6 ( $^2J_{\text{C,P}} = 5.4$ Hz)
4	19.2	16.0

<sup>a</sup> From Marsden et al. (1989). <sup>b</sup> In D<sub>2</sub>O, as a dimer.

additional low-field resonances appear at 103.4, 142.3, 152.5, and 166.8 ppm, which are attributed to the uracil ring. Five carbonyl resonances are present, two of which are assigned to two *N*-acetyl groups, two to the acid functions of heptanoic acid and phosphothreonine, and one to the mannuronic acid moiety. Two resonances appear at ~54 ppm, which are characteristic of *N*-acetylated sugars, one of which appears to be phosphorus coupled ( $J_{\text{C,P}} = 9.0$  ppm). The high-field portion of the spectrum showed the presence of six methylene carbon resonances between 24 and 36 ppm, two *N*-acetyl methyl resonances at 22.7 ppm, and one additional methyl resonance at 19.2 ppm. The resonances of MRF were assigned by comparison to the previously assigned  $^{13}\text{C}$  spectrum of the carbohydrate moiety (Marsden et al., 1989) and the spectra of synthetic HS-HTP and an authentic sample of UDP-GlcNAc. The latter was unambiguously assigned by using an  $^1\text{H}$ - $^{13}\text{C}$  correlation (HETCOR) spectrum. The  $^1\text{H}$  and  $^{13}\text{C}$  resonance assignments of these four compounds are summarized in Tables I and II. In the spectrum of MRF, eight of the carbon resonances showed coupling to phosphate moieties. These occurred at 54.1, 64.4, 65.5, 72.8, 77.8, 83.8, 95.5, and 176.3 ppm and indicate the presence of two and possibly three phosphate linkages within the intact MRF molecule.

The  $^{31}\text{P}$  NMR spectra of UDP-GlcNAc-ManNAcA and MRF are compared in Figure 2. The  $^{31}\text{P}$  NMR spectrum

FIGURE 2:  $^{31}\text{P}$  NMR spectra, 202 MHz, of (A) MRF and (B) UDP-GlcNAc-ManNAcA.

of MRF (Figure 2A) shows three resonances at -10.6, -12.4, and 1.3 ppm, indicating the presence of three phosphate groups; two in a pyrophosphate linkage and one mono-

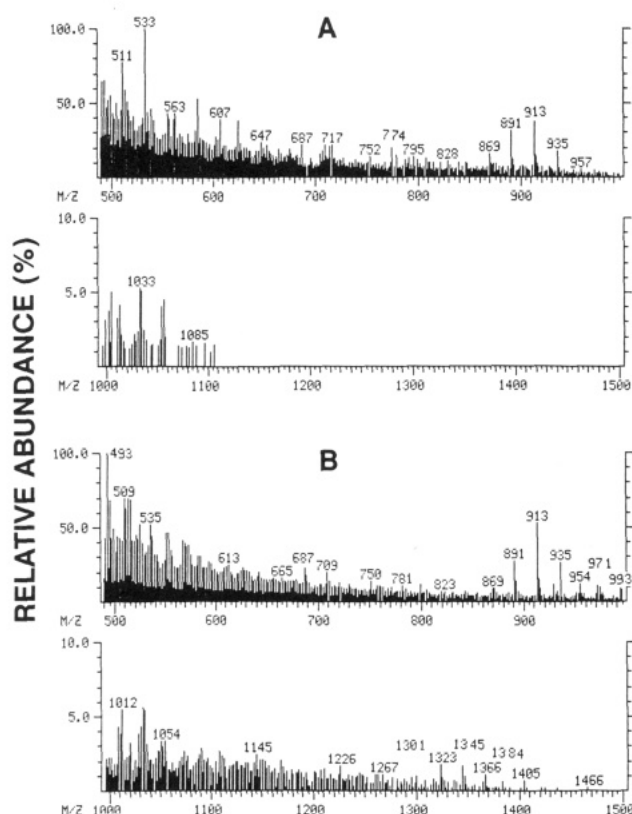


FIGURE 3: FAB-MS of UDP-GlcNAc-ManNAcA dissolved in a glycerol matrix (A); FAB-MS of MRF dissolved in thioglycerol (B).

phosphate with a 1:1:1 intensity ratio. The other monophosphate resonances of smaller intensity are assigned to HS-HTP (by comparison with the  $^{31}\text{P}$  NMR spectrum of synthetic HTP-S-S-HTP, which has a single phosphate resonance at 2.3 ppm), free phosphothreonine (identified by titration), and a small amount of free phosphate. The  $^{31}\text{P}$  NMR spectrum of UDP-GlcNAc-ManNAcA (Figure 2B) shows the pyrophosphate doublets at -10.4 and -12.1 ppm with a phosphorus-phosphorus coupling of 20 Hz, as previously described (Marsden et al., 1989). The small monophosphate resonance (1.3 ppm) is due to the presence of a small amount of residual, intact MRF. These data, combined with the  $^{13}\text{C}$  data, indicate that the individual moieties of the intact MRF molecule, namely, the mercaptoheptanoic acid, *O*-phosphothreonine, uridine, and the carbohydrate moieties, are linked by phosphate groups.

Figure 3 shows the FAB-MS of UDP-GlcNAc-ManNAcA and MRF. The molecular ion of the Na salt of the UDP-disaccharide  $[\text{M}(3\text{Na}) + \text{H}]^+$  occurred at  $m/z$  891 (theoretical

$m/z$  891.09). Loss of one  $\text{Na}^+$   $[\text{M}(2\text{Na},\text{H}) + \text{H}]^+$  gave  $m/z$  869 (theoretical  $m/z$  869.11). The Na salt with  $\text{Na}^+$   $[\text{M}(3\text{Na}) + \text{Na}]^+$  gave  $m/z$  913 (theoretical  $m/z$  913.07), with two  $\text{Na}^+$   $[\text{M}(3\text{Na}) + 2\text{Na}-\text{H}]^+$  gave an  $m/z$  935 (theoretical  $m/z$  935.06).

The molecular ion of MRF was only obtained by using thioglycerol as a matrix for the FAB-MS. The use of glycerol and the addition of acetic acid, HCl, or oxalic acid to the glycerol (or thioglycerol) matrix, caused extensive breakup of the molecule during FAB-MS indicating that MRF is very sensitive to acid degradation. MRF was isolated as the heterodisulfide of 2-mercaptoethanol, but during FAB-MS analysis, the mercaptoethanol exchanged for thioglycerol.

The molecular ion of the Na salt of the thioglycerol derivative of MRF occurred at  $m/z$  1345  $[\text{M}(4\text{Na}) + \text{H}]^+$  (theoretical  $m/z$  1344.16) (Figure 3B). The molecular ion displayed a characteristic loss of one  $\text{Na}^+$  ( $m/z$  1323; theoretical  $m/z$  1322.18  $[\text{M}(3\text{Na},\text{H}) + \text{H}]^+$ ) or two  $\text{Na}^+$  ( $m/z$  1301; theoretical  $m/z$  1300.19  $[\text{M}(2\text{Na},2\text{H}) + \text{H}]^+$ ) or an addition of one  $\text{Na}^+$  ( $m/z$  1367; theoretical  $m/z$  1366.14  $[\text{M}(4\text{Na}) + \text{Na}]^+$ ).

A major cleavage of MRF (Figure 4) occurred at the anhydride linkage, giving rise to the peak at  $m/z$  493 (I, theoretical  $m/z$  493.06), which represents the disulfide oxidation product of HS-HTP and thioglycerol. Another cleavage occurred between the  $\beta$ -link of ManNAcA and GlcNAc to yield a fragment at  $m/z$  709 (II, theoretical  $m/z$  709.11) with adjacent peaks dependent on the addition or loss of  $\text{Na}^+$ . The ion at  $m/z$  913 (theoretical  $m/z$  913.19) can arise in two ways: by the formation of the Na salt of UDP-GlcNAc-ManNAcA (Marsden et al., 1989) or by breakage adjacent to the pyrophosphate moiety. The breakup pattern from the UDP end of the molecule results in cleavage ions at  $m/z$  954 (IV, theoretical  $m/z$  954.06) and at  $m/z$  970 (V, theoretical  $m/z$  970.05). Each of the fragment ions showed evidence of loss of one or two or gain of one  $\text{Na}^+$  atom(s) to give typical ion clusters. These ions, produced from opposite ends of the molecule, account for the complete structure of MRF, which consists of covalently linked UDP-GlcNAc-ManNAcA and HS-HTP. From the above data, MRF was identified as uridine 5'-[*N*-(7-mercaptoheptanoyl)-*O*-3-phosphothreonine-*P*-yl(2-acetamido-2-deoxy- $\beta$ -mannopyranuronosyl)(acid anhydride)]-(1 $\rightarrow$ 4)-*O*-2-acetamido-2-deoxy- $\alpha$ -glucopyranosyl diphosphate (Figure 4).

From the hyperbolic plots of methane production rates versus concentrations of HS-HTP or MRF, the data points were recalculated from Eadie and Hofstee plots. From data fitted by the least-squares method,  $V_{\text{max}}$  for MRF and HS-HTP was 124 and 83 nmol of  $\text{CH}_4 \text{ min}^{-1} (\text{mg of protein})^{-1}$ ,

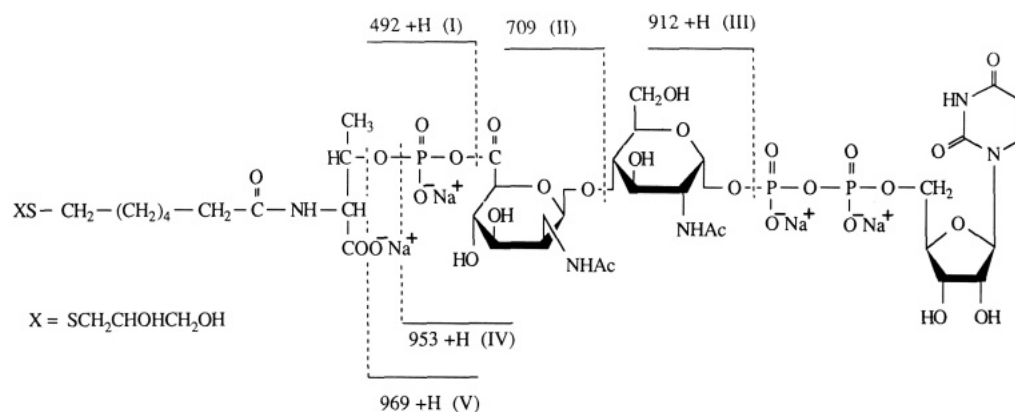


FIGURE 4: Chemical structure of MRF showing some of the major fragmentation ions produced during FAB-MS.

Table III: Addition of UDP-GlcNAc-ManNAcA to the Methylcoenzyme M Methylreductase Reaction<sup>a</sup>

UDP-GlcNAc-ManNAcA concn ( $\mu$ M)	CH <sub>4</sub> synthesis (nmol)
0	646
22	643
42	635
84	660
168	632

<sup>a</sup>Incubations were carried out as described under Materials and Methods. The fractions were incubated in the presence of 2.75 mM HS-HTP.

respectively, with a  $K_{m(\text{app})}$  for MRF and HS-HTP respectively of 115 and 660  $\mu$ M.

Since MRF stimulated the methylcoenzyme M methylreductase reaction more than HS-HTP, it was of interest to determine if the carbohydrate moiety of MRF was by itself stimulatory in methylcoenzyme M reduction. As shown in Table III, methylcoenzyme M methylreductase activity in the presence of an excess concentration (i.e., nonlimiting) of HS-HTP was not increased by concentrations of UDP-GlcNAc-ManNAcA up to 168  $\mu$ M.

## DISCUSSION

In determining the structure of MRF, we first isolated and purified the UDP-GlcNAc-ManNAcA carbohydrate moiety of MRF and elucidated its structure by a combination of <sup>1</sup>H, <sup>13</sup>C, and <sup>31</sup>P NMR and FAB-MS (Marsden et al., 1989). We presented evidence that is consistent with the UDP-disaccharide having the following structure: UDP- $\alpha$ -GlcNAc-(4 $\rightarrow$ 1)- $\beta$ -ManNAcA.

Two publications have appeared recently that propose different structures for the UDP-disaccharide isolated from *Mb. thermoautotrophicum* (König et al., 1989; Keltjens et al., 1989). König et al. (1989) isolated a disaccharide moiety from trichloroacetic acid extracts of *Mb. thermoautotrophicum* and reported that it was composed of GlcNAc and TalNAcA. The anomeric configuration of the two sugars was reported as being  $\alpha$  and  $\beta$ , respectively, but the position of the glycosidic linkage of the TalNAcA residue was not reported.

The structure proposed by Keltjens et al. (1989) for UDP-GlcNAc-ManNAcA agrees with our result except for the position of the glycosidic linkage of the ManNAcA residue. They reported a 1-3 linkage whereas we propose that it is 1-4.

To clarify these discrepancies, we have performed a spectral simulation of the <sup>1</sup>H NMR spectrum of the UDP-disaccharide (Figure 5). This spectral simulation permits refinement in the determination of the proton chemical shifts and coupling constants and the results are consistent with the previous resonance assignments (Marsden et al., 1989). Both the simulated and observed spectra are shown in Figure 5 and the derived proton chemical shifts and coupling constants are given in Table I.

The structure of mannose and talose differ only in the configuration at C-4. It is therefore possible to differentiate these two configurations on the basis of the <sup>1</sup>H-<sup>1</sup>H coupling constants between H-3 and H-4 and between H-4 and H-5 (<sup>3</sup>J<sub>3,4</sub> and <sup>3</sup>J<sub>4,5</sub>, respectively). The <sup>3</sup>J<sub>3,4</sub> and <sup>3</sup>J<sub>4,5</sub> coupling constant values for  $\beta$ -D-mannopyranose are 10.0 and 9.8 Hz, respectively (Bock and Thorgensen, 1982), while the values for  $\beta$ -D-talopyranose are 3.3 and 1.2 Hz, respectively (Snyder et al. 1989). The observed values for <sup>3</sup>J<sub>3,4</sub> of 9.86 Hz and for <sup>3</sup>J<sub>4,5</sub> of 9.87 Hz are in good agreement with  $\beta$ -D-mannopyranose and thus confirm the configuration.

A 1-D rOe difference spectrum (Figure 6) provides information that can be used to determine the sequence of the

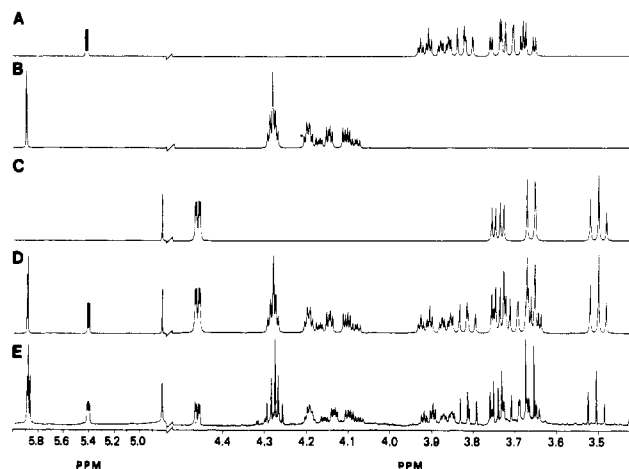


FIGURE 5: Spectral simulation, 500 MHz, of the carbohydrate region of UDP-GlcNAc-ManNAcA. (A) Glucose residue; (B) ribose residue; (C) mannose residue; (D) sum of (A), (B), and (C); and (E) the 500-MHz single-pulse spectrum. Coupling constants and chemical shifts used in the spectral simulation were as given in Table I.

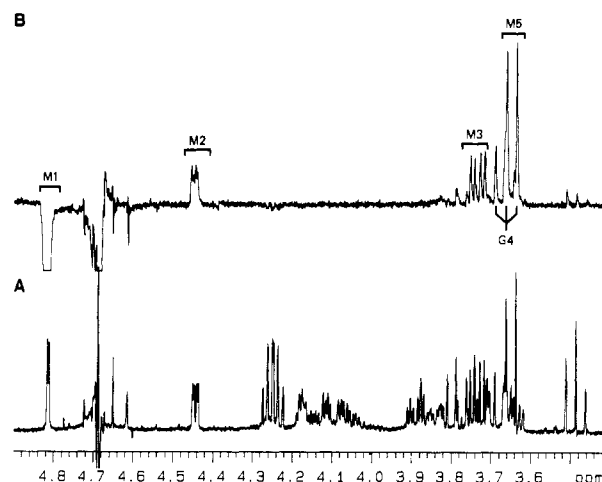


FIGURE 6: 1-D rOe difference spectrum of UDP-GlcNAc-(4 $\rightarrow$ 1)-ManNAcA. (A) Normal spectrum; (B) selective excitation of the proton resonance of ManNAcA. Spectra were acquired on a Varian VXR-400S NMR spectrometer operating at 399.95 MHz and 25 °C; a spin lock period of 250 ms was used. See Figure 1 for notation.

monosaccharides. This technique permits the observation of the resonances of only those protons that are in close proximity ( $\leq 3$  Å) to the proton whose signal has been moderated. Irradiation of the H-1 of the ManNAcA produced rOe's on H-2, H-3, and H-5 of the ManNAcA residue in addition to an rOe on H-4 of the GlcNAc residue. This indicates that the ManNAcA residue is glycosidically linked to the C-4 position of the GlcNAc residue. This result confirms that which was reported earlier (Marsden et al. 1989), using <sup>13</sup>C NMR data. Keltjens et al. (1989) made their assignment based on a comparison of the changes in chemical shift of the <sup>1</sup>H resonances H-3 and H-4 of UDP-GlcNAc disaccharide and UDP-GlcNAc. It is well-known that the assignment of the position of a glycosidic linkage using changes in <sup>1</sup>H NMR chemical shift data is less sensitive than the changes observed in the <sup>13</sup>C NMR chemical shift (Perlin & Casu, 1982). Also, the changes observed in the <sup>1</sup>H NMR chemical shifts are dependent on the position of the linkage. This would explain why Keltjens et al. (1989) have incorrectly assigned the glycosidic linkage.

Comparison of the <sup>13</sup>C spectral assignments of the UDP-GlcNAc and the carbohydrate moiety (Table II) provide further evidence of substitution at the 4-position of GlcNAcA.

The  $\alpha$ -effect of substitution on C-4 causes a downfield shift of 10 ppm, with a  $\beta$ -effect of 0.8–1.0 ppm downfield shift at C-3 and C-5, as would be expected with substitution at this position. The remaining resonances between these two species are comparable.

MRF has the phosphate group of HS-HTP bound to UDP-GlcNAc-ManNAcA through a mixed-anhydride linkage to the C-6 of ManNAcA. It is recognized that carboxylic-phosphoric anhydrides are susceptible to nonenzymatic hydrolysis at below pH 5 or above pH 10, particularly in the presence of divalent cations, i.e.,  $\text{Ca}^{2+}$  or  $\text{Mg}^{2+}$  (Koshland, 1951). In a similar manner, the unusual mixed anhydride in MRF can be hydrolyzed by dilute acids and relatively mild isolation and purification procedures. MRF, however, can be separated from HS-HTP by silica gel TLC, paper chromatography, or electrophoresis and column chromatography with hydroxylapatite, provided all buffers are kept near pH 7. MRF undergoes partial hydrolysis during DEAE-Sephadex chromatography and samples used for NMR spectroscopy sometimes contained free UDP-GlcNAc-ManNAcA in addition to MRF.

The structure of intact MRF was deduced from FAB-MS and  $^{13}\text{C}$  NMR data. During FAB-MS, the breakup pattern of MRF yielded readily identifiable fragment ions both from the uracil end and the HS-HTP end of the molecule, with each of the fragment ions showing evidence for either the loss of one or two or the gain of one  $\text{Na}^+$  atom(s) to give typical ion clusters. These ions, produced from opposite ends of the molecule, give unequivocal support for the proposed structure of MRF. The molecular ion of the Na salt of the thioglycerol derivative of MRF  $[\text{M}(4\text{Na}) + \text{H}]^+$  occurred at  $m/z$  1345 (theoretical  $m/z$  1344.16). MRF may exist naturally as the Na salt because as isolated it is saturated with  $\text{Na}^+$  atoms. The molecular formula of MRF is  $\text{C}_{36}\text{H}_{58}\text{O}_{29}\text{N}_5\text{P}_3\text{S}_1$  with  $M_r$  1149.21.

The  $^{13}\text{C}$  NMR data provide convincing evidence for the acid anhydride linkage between the phosphate group of HS-HTP and C-6 of ManNAcA. The carbon chemical shift assignments of UDP-GlcNAc-ManNAcA, both in the free state and when bonded to HS-HTP, are compared in Figure 1. In the MRF and UDP-GlcNAc-ManNAcA mixture (Figure 1B), the resonances due to UDP-GlcNAc-ManNAcA can be assigned by direct comparison to the spectrum of Figure 1A. As can be noted, the acid anhydride linkage results in a shifting of the resonances of most carbon atoms except for those due to carbon atoms removed from C-6 of ManNAcA (for example, C-2 and C-3 of ribose and C-3 and C-4 of glucose). Slight changes in chemical shift ( $\sim 0.2$  ppm) are noted for some uracil ring resonances (Table II), which may relate to the conformational differences between the bound and the free UDP-GlcNAc-ManNAcA moiety. The most significant NMR data in favor of a carboxylic-phosphoric anhydride bond between C-6 of ManNAcA and HS-HTP was from the appearance of splitting due to carbon-phosphorus coupling on the C-5 and C-6 resonances of ManNAcA. In the free UDP-GlcNAc-ManNAcA moiety, these resonances appear as singlets at 77.6 and 176.4 ppm, respectively, whereas in the spectrum of MRF, these resonances are shifted to 77.8 and 176.3 ppm and appear as doublets ( $^3J_{\text{CP}} = 5.7$  Hz and  $^2J_{\text{CP}} = 7.2$  Hz). Furthermore, the resonances due to HS-HTP, specifically those of phosphothreonine, are shifted downfield in intact MRF.

The  $^{31}\text{P}$  and  $^1\text{H}$  NMR spectra are also consistent with the chemical structure of MRF. The  $^1\text{H}$  NMR spectrum (Table I) of MRF shows the presence of all the resonances due to

UDP-GlcNAc-ManNAcA and HS-HTP, in which the resonances due to H-4 and H-5 of the ManNAcA residue are only slightly affected (0.05 ppm) by the phosphate linkage. The most significant change occurs for the resonance due to H-3 of threonine, which has shifted downfield by 0.5 ppm. In the well-resolved portion of the spectrum, even the resonance due to the anomeric proton of GlcNAc in the intact MRF can be distinguished by a downfield shift of  $\sim 0.05$  ppm from that in UDP-GlcNAc-ManNAcA. The stoichiometric ratio of the three phosphate resonances assigned to the pyrophosphate and disubstituted monophosphate groups of MRF is evident from the  $^{31}\text{P}$  NMR data (Figure 2). In addition, the monophosphate resonance of MRF (1.3 ppm) shows a 1.0 ppm shift from that of free HS-HTP (2.3 ppm).

The  $K_{\text{m}(\text{app})}$  of methylcoenzyme M methylreductase for MRF is approximately 6-fold lower than for HS-HTP and with a 50% increase in  $V_{\text{max}}$ . Keltjens et al. (1989) reported that methanogenesis was stimulated above base levels by the addition of only the carbohydrate moiety, UDP-GlcNAc-ManNAcA. This was not supported by our experiments in which UDP-GlcNAc-ManNAcA, at concentration of 22–168  $\mu\text{M}$  neither stimulated nor inhibited the rates of methanogenesis. In the high-resolution 500-MHz  $^1\text{H}$  NMR spectrum of UDP-GlcNAc-ManNAcA published by Keltjens et al. (1989), traces of HS-HTP are clearly visible. It is possible that the stimulation of methanogenesis attributed by these authors to UDP-GlcNAc-ManNAcA is in fact due to residual traces of MRF present in their preparation. The biosynthesis and function of MRF are currently under investigation.

#### ACKNOWLEDGMENTS

The expert technical assistance of Mr. P. Lafontaine for performing FAB mass spectrum analyses is acknowledged.

**Registry No.** MRF, 128218-31-5; UDP-GlcNAc-ManNAcA, 123940-49-8; methylcoenzyme M methylreductase, 53060-41-6.

#### REFERENCES

- Bax, A., & Freeman, R. (1981) *J. Magn. Reson.* **44**, 542–561.
- Bax, A., & Drobny, G. (1985) *J. Magn. Reson.* **61**, 306–320.
- Bock, K., & Thorgensen, H. (1982) in *Annual Reports on Nuclear Magnetic Resonance Spectroscopy* (Webb, G. A., Ed.) pp 1–57, Academic Press, London, U.K.
- Keltjens, J. T., Kraft, H. J., Damen, W. G., van der Drift, C., & Vogels, G. D. (1989) *Eur. J. Biochem.* **184**, 395–403.
- Kessler, H., Griesinger, C., Kerssebaum, R., Wagner, K., & Ernst, R. R. (1987) *J. Am. Chem. Soc.* **109**, 607–609.
- König, H., Kandler, O., & Hammes, W. (1989) *Can. J. Microbiol.* **35**, 176–181.
- Koshland, D. E. (1951) *J. Am. Chem. Soc.* **74**, 2286–2292.
- Marsden, B. J., Sauer, F. D., Blackwell, B. A., & Kramer, J. K. G. (1989) *Biochem. Biophys. Res. Commun.* **159**, 1404–1410.
- Mayer, F., Rohde, M., Salzmann, M., Jussofie, A., & Gottschalk, G. (1988) *J. Bacteriol.* **170**, 1438–1444.
- Noll, K. M., & Wolfe, R. S. (1986) *Biochem. Biophys. Res. Commun.* **139**, 889–895.
- Noll, K. M., Rinehart, K. L., Tanner, R. S., & Wolfe, R. S. (1986) *Proc. Natl. Acad. Sci. U.S.A.* **83**, 4238–4242.
- Pearson, G. A. (1985) *J. Magn. Reson.* **64**, 487–500.
- Perlin, A. S., & Casu, B. (1982) in *The Polysaccharides* (Aspinall, O. E., Ed.) Vol. 1, pp 133–195, Academic Press, London, U.K.
- Sauer, F. D., Mahadevan, S., & Erfle, J. D. (1984) *Biochem. J.* **221**, 61–69.



- Sauer, F. D., Blackwell, B. A., & Mahadevan, S. (1986) *Biochem. J.* 235, 453-458.  
 Sauer, F. D., Blackwell, B. A., & Kramer, J. K. G. (1987) *Biochem. Biophys. Res. Commun.* 147, 1021-1026.

- Shaka, A. J., & Freeman, R. (1983) *J. Magn. Reson.* 51, 169-173.  
 Snyder, J. R., Johnston, E. R., & Serrianni, A. S. (1989) *J. Am. Chem. Soc.* 111, 2681-2687.

## Structure of Chymotrypsin-Trifluoromethyl Ketone Inhibitor Complexes: Comparison of Slowly and Rapidly Equilibrating Inhibitors<sup>†</sup>

Kenneth Brady,<sup>‡</sup> Anzhi Wei,<sup>§</sup> Dagmar Ringe,<sup>||</sup> and Robert H. Abeles<sup>\*||</sup>

Department of Toxicology, Harvard School of Public Health, 665 Huntington Avenue, Boston, Massachusetts 02115, Department of Chemistry, University of Pennsylvania, Philadelphia, Pennsylvania 19104-6323, and Graduate Department of Biochemistry, Brandeis University, 415 South Street, Waltham, Massachusetts 02254

Received December 27, 1989; Revised Manuscript Received May 2, 1990

**ABSTRACT:** The peptidyl trifluoromethyl ketones Ac-Phe-CF<sub>3</sub> (**1**) and Ac-Leu-Phe-CF<sub>3</sub> (**2**) are inhibitors of chymotrypsin. They differ in  $K_i$  (20 and 2  $\mu$ M, respectively) as well as in their kinetics of association with chymotrypsin in that **1** is rapidly equilibrating, with an association rate too fast to be observed by steady-state techniques, while **2** is "slow binding", as defined by Morrison and Walsh [Morrison, J. F., & Walsh, C. T. (1988) *Adv. Enzymol. Relat. Areas Mol. Biol.* 61, 202], with a second-order association rate constant of 750 M<sup>-1</sup> s<sup>-1</sup> at pH 7.0 [Imperiali, B., & Abeles, R. (1986) *Biochemistry* 25, 3760]. The crystallographic structures of the complexes of  $\gamma$ -chymotrypsin with inhibitors **1** and **2** have been determined in order to establish whether structural or conformational differences can be found which account for different kinetic and thermodynamic properties of the two inhibitors. In both complexes, the active-site Ser 195 hydroxyl forms a covalent hemiketal adduct with the trifluoromethyl ketone moiety of the inhibitor. In both complexes, the trifluoromethyl group is partially immobilized, but differences are observed in the degree of interaction of fluorine atoms with the active-site His 57 imidazole ring, with amide nitrogen NH 193, and with other portions of the inhibitor molecule. The enhanced potency of Ac-Leu-Phe-CF<sub>3</sub> relative to Ac-Phe-CF<sub>3</sub> is accounted for by van der Waals interactions of the leucine side chain of the inhibitor with His 57 and Ile 99 side chains and by a hydrogen bond of the acetyl terminus with amide NH 216 of the enzyme. It is likely that the slower association rate of **2** with chymotrypsin as well as the lower  $K_i$  can be accounted for by the interaction of the P<sub>2</sub> (Leu) substituent. No major differences in protein conformation between the two complexes were observed. Upon dissolution of crystalline chymotrypsin-Ac-Leu-Phe-CF<sub>3</sub> into buffer, inhibitor is observed to dissociate from the complex at the same rate as observed for the enzyme-inhibitor complex which has been formed in solution, indicating that the complex studied crystallographically is probably identical with the complex which has been studied in solution [Imperiali, B., & Abeles, R. (1986) *Biochemistry* 25, 3760; Liang, T.-C., & Abeles, R. H. (1987) *Biochemistry* 26, 7603; Brady, K., Liang, T.-C., & Abeles, R. H. (1989) *Biochemistry* 28, 9066; K. Brady and R. H. Abeles, submitted for publication].

**P**eptidyl trifluoromethyl ketones are inhibitors of serine proteases. By analogy with the peptidyl aldehydes (Delbaere & Brayer, 1985; Thompson & Bauer, 1979), the nucleophilic serine of the enzyme is believed to add to the highly electrophilic trifluoromethyl ketone moiety to form a stable hemiketal adduct. Specificity and potency are provided by linking oligopeptides to the core ketone moiety in a manner analogous to improving the kinetic specificity of substrates by peptide extension (Bauer, 1978). Peptidyl trifluoromethyl ketones have been studied as inhibitors of chymotrypsin, elastase (Imperiali & Abeles, 1986; Stein et al., 1987),  $\alpha$ -lytic protease (Go-

vardhan, unpublished results), trypsin, and thrombin (Liang and Abeles, unpublished results) with equilibrium dissociation constants ( $K_i$ ) in the micromolar to subnanomolar range.

Many peptidyl trifluoromethyl ketones are "slow-binding"<sup>1</sup> (Morrison & Walsh, 1988) inhibitors. Second-order rates of association ( $k_{on}$ ) of peptidyl trifluoromethyl ketones with serine proteases have been measured in the range 700-80 000 M<sup>-1</sup> s<sup>-1</sup> (Imperiali & Abeles, 1986; Stein et al., 1987), with rates varying as a function of peptide length and composition. Slow

<sup>†</sup> Publication No. 1711 of the Graduate Department of Biochemistry, Brandeis University. This research is supported by NIH Grant GM 12633-25 to R.H.A.

\* Address correspondence to this author.

<sup>‡</sup> Harvard School of Public Health.

<sup>§</sup> University of Pennsylvania.

<sup>||</sup> Brandeis University.

<sup>1</sup> Although the term slow binding is useful for the classification of inhibitors, it is not helpful in leading to an understanding of the mechanism of enzyme-inhibitor interaction. The association constant of enzyme and inhibitor and the dissociation constant of the enzyme-inhibitor complex are more informative. Some, but not all, slow-binding inhibitors actually have slow association constants ( $\ll 10^7$  M<sup>-1</sup> s<sup>-1</sup>). For the inhibitors under discussion,  $k_{on} = 700$  M<sup>-1</sup> s<sup>-1</sup> and  $k_{off} = 0.0017$  for **2**, and  $k_{on} = 3010$  M<sup>-1</sup> s<sup>-1</sup> and  $k_{off} = 0.065$  s<sup>-1</sup> for **1** (Brady and Abeles, unpublished results).